Molecular Ecology (2007) **16**, 3995–4013 doi: 10.1111/j.1365-294X.2007.03445.x

Diversity and divergence patterns in regulatory genes suggest differential gene flow in recently derived species of the Hawaiian silversword alliance adaptive radiation (Asteraceae)

A. LAWTON-RAUH,* R. H. ROBICHAUX† and M. D. PURUGGANAN‡§
*Department of Genetics and Biochemistry, Clemson University, 100 Jordan Hall, Clemson, SC 29634-0318, USA, †Department of Ecology and Evolutionary Biology, University of Arizona, Tucson, AZ 85721, USA, ‡Department of Genetics, North Carolina State University, Box 7614, Raleigh, NC 27695-7614, USA

Abstract

The impact of gene flow and population size fluctuations in shaping genetic variation during adaptive radiation, at both the genome-wide and gene-specific levels, is very poorly understood. To examine how historical population size and gene flow patterns within and between loci have influenced lineage divergence in the Hawaiian silversword alliance, we have investigated the nucleotide sequence diversity and divergence patterns of four floral regulatory genes (*ASAP1-A*, *ASAP1-B*, *ASAP3-A*, *ASAP3-B*) and a structural gene (*ASCAB9*). Levels and patterns of molecular divergence across these five nuclear loci were estimated between two recently derived species (*Dubautia ciliolata* and *Dubautia arborea*) which are presumed to be sibling species. This multilocus analysis of genetic variation, haplotype divergence and historical demography indicates that population expansion and differential gene flow occurred subsequent to the divergence of these two lineages. Moreover, contrasting patterns of allele- sharing for regulatory loci vs. a structural locus between these two sibling species indicate alternative histories of genetic variation and partitioning among loci where alleles of the floral regulatory loci are shared primarily from *D. arborea* to *D. ciliolata* and alleles of the structural locus are shared in both directions. Taken together, these results suggest that adaptively radiating species can exhibit contrasting allele migration rates among loci such that allele movement at specific loci may supersede genetic divergence caused by drift and that lineage divergence during adaptive radiation can be associated with population expansion.

Keywords: adaptive radiation, allele-sharing, gene flow, Hawaiian silversword alliance, regulatory gene evolution, speciation

Received 19 November 2006; revision accepted 4 June 2007

The processes underlying adaptive evolution and lineage differentiation act in concert to yield the most dramatic examples of organismal diversification: adaptive radiations. Adaptive radiations are rapidly evolving species groups that have undergone adaptive ecological differentiation correlated with elevated morphological and physiological divergence among lineages (Schluter 2000). Several of the most studied dramatic examples of adaptive radiation include Darwin's finches on the Galapagos Islands (Lack 1947; Grant 1986; Grant & Grant 1994), West Indian *Anolis* lizards on the Caribbean Islands (Irschick *et al*. 1998; Losos & Miles 2002), columbines in North America (*Aquilegia*) (Chase & Raven 1975; Miller 1981; Hodges 1997; Fulton & Hodges 1999), and the Hawaiian silversword alliance (Carr 1985; Robichaux *et al*. 1990; Baldwin & Sanderson 1998, reviewed in Schluter 2000).

Most studies of adaptive radiations focus on the macro-evolutionary effects of rapid phenotypic evolution and

Correspondence: Amy Lawton-Rauh, Fax: 864-656-6879; E-mail: AmyLR@clemson.edu
§Present address: Department of Biology, 1009 Main Building, 100 Washington Square East, New York University, New York, NY 10003-6688, USA.

correlations of measurable phenotypes with trait utility and divergence between species (Schluter 2000). Relatively little is known, however, about genetic variation among diverging lineages and the historical impact of demographic factors in adaptive radiations. These demographic factors include population size fluctuations due to changes in range availability, and gene flow between diverging lineages. Such factors are expected to directly impact the mode and tempo of diversification, especially in the rapid evolutionary timescales associated with the accelerated speciation rates of adaptive radiations.

Demographic forces affect genome-wide levels and patterns of genetic variation and remain difficult to distinguish from the signatures of natural selection on specific loci. In general, demographic forces affect every locus in the genome and impact genome-wide estimates of effective population size. Additionally, demographic effects (gene flow in particular) may, in some cases, actually reinforce lineage divergence by acting as a mechanism promoting locus-specific allelic differentiation through local adaptation (Caisse & Antonovics 1978; Church & Taylor 2002; Rieseberg *et al*. 2004).

Inferring the impact of demographic forces is facilitated by recent advances in molecular population genetic analyses, including Bayesian and Markov chain Monte Carlo analytical approaches (Kuhner *et al*. 1998; Beerli & Felsenstein 1999; Nielsen & Wakeley 2001; Rannala & Yang 2003; Wang & Whitlock 2003; Zheng *et al*. 2003; Hey & Nielsen 2004), which examine multilocus patterns of nucleotide polymorphisms shaped by historical events that affect the entire genome. These approaches have been employed in a variety of areas, including reconstruction of phylogeographic divergences among taxonomic lineages (Yoder & Yang 2004), assessing conservation strategies for sea fin whales (Palsboll *et al*. 2004), Hawaiian groupers (Rivera *et al*. 2004), and grasshopper sparrows (Bulgin *et al*. 2003), as well as studying the historical divergence population genetics in the *Drosophila* genus (Hey & Nielsen 2004) and among African cichlids (Hey *et al*. 2004).

We have utilized population genetic approaches to examine the extent of morphological and molecular differentiation associated with speciation within the Hawaiian silversword alliance (Asteraceae–Madiinae). Numerous studies have explored the phylogeny (Baldwin *et al*. 1991; Baldwin & Sanderson 1998; Barrier *et al*. 1999; Baldwin & Wessa 2000), cytogenetics (Carr 1978; Carr & Kyhos 1981; Carr 1985), physiological ecology (Robichaux 1984; Robichaux & Canfield 1985; Robichaux *et al*. 1990) and conservation genetics of the silversword alliance (Friar *et al*. 1996, 2000, 2001; Robichaux *et al*. 1997), yet the variance underlying molecular and morphological diversification during speciation within the Hawaiian silversword alliance remains unclear. This molecular population genetic analysis of several floral regulatory genes and a structural gene in two recently derived species of the silversword alliance provides unique insights into the differential impact of demographic forces across functional loci during the origin and establishment of members of this adaptive radiation. Additionally, this approach permits an assessment of historical population dynamics underlying the rapid speciation processes responsible for the phenotypic variation displayed among the Hawaiian silversword alliance species and provides clues regarding potential multilocus as well as locus-specific mechanisms partitioning lineages during adaptive evolution.

The Hawaiian silversword alliance

The Hawaiian silversword alliance, which is believed to rank 'with the dinosaur extinctions and the origin of our own species (as) among the most celebrated events in the history of life' (Schluter 2000), consists of 30 species in three genera (*Argyroxiphium*, *Wilkesia*, and *Dubautia*) endemic to the Hawaiian archipelago (Carr 1985). Silversword alliance species exhibit remarkable morphological and ecological differentiation and are extensively described elsewhere (see, for example: Carr 1985; Robichaux *et al*. 1990; Baldwin & Robichaux 1995; Baldwin 1997). Previous analyses of 10 allozyme loci indicate low genetic differentiation among Hawaiian silversword alliance species (Witter & Carr 1988). Furthermore, even species that diverged approximately 5.2 to 1.5 million years ago (Ma) have highly similar genetic identities, with many Nei genetic identity coefficients in the range of values expected between intraspecific populations ($I > 0.90$; Nei 1972; Witter & Carr 1988).

This study focuses on two recently derived species (*Dubautia ciliolata* subsp. *glutinosa* and *Dubautia arborea*) in the Railliardia lineage of the Hawaiian silversword alliance that are endemic to the island of Hawaii (Carr 1985; Baldwin 1997) and exhibit different growth forms and reproductive architecture features both in the field and in common garden experiments (see Fig. 1; Carr 1985; Robichaux *et al*. 1990). Phylogenetic analysis indicates that both *D. ciliolata* subsp. *glutinosa* and *D. arborea* are likely sibling species, and their endemism on the youngest island of the archipelago suggests that these two species diverged from each other after the origin of this island approximately 0.5 Ma (Carson & Clague 1995). To examine ancestral vs. derived variation and to cover the temporal breadth of the adaptive radiation, this study also includes *Argyroxiphium sandwicense* subsp. *macrocephalum*, which is in the Argyroxiphium lineage of the Hawaiian silversword alliance and is endemic to Haleakala volcano on Maui.

Inferences of historical demography associated with species differentiation are best accomplished using locus-specific and combined multilocus analyses. This approach makes it possible to examine single-locus and multilocus patterns consistent with demographic models. Additionally,

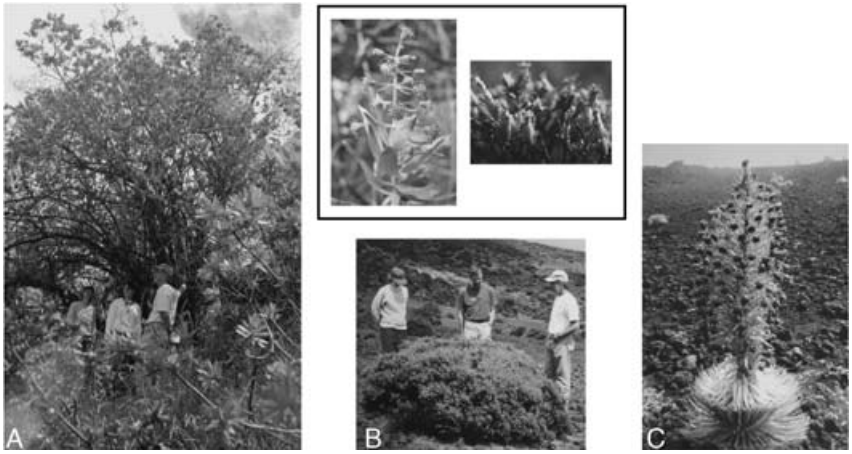

Fig. 1 Approximate relative growth form sizes among *Dubautia arborea* (A), *Dubautia ciliolata* subsp. *glutinosa* (B) on Mauna Kea, Hawaii and *Argyroxiphium sandwicense* ssp. *macrocephalum* (C) in Haleakala crater, Maui. Inflorescence architecture comparison (see inset) between *D. arborea* (single capitulescence shown, left) and *Dubautia ciliolata* (multiple capitulescences, each with solitary capitula shown, right). Photo A courtesy of David Remington and *D. arborea* inflorescence photo in inset courtesy of Gerald Carr.

comparing loci of different functional classes provides the opportunity to set up hypotheses that can be more thoroughly addressed using further data sets regarding processes partitioning evolutionary forces across loci. Several nuclear genes have been isolated from members of the Hawaiian silversword alliance and can be used to assess multilocus patterns of nucleotide polymorphisms in these species. The homeologous regulatory genes *ASAP1-A* and *-B* and *ASAP3/TM6-A* and *-B* as well as the chlorophyll A/B binding protein encoding gene *ASCAB9* were used in this study. All five of these loci have been used in other molecular evolutionary studies of the Hawaiian silversword alliance (Barrier *et al*. 2001). The floral regulatory genes in this study represent functional loci undergoing accelerated rates of evolution (Barrier *et al*. 2001) and divergent evolutionary trajectories between homoeologs (Lawton-Rauh *et al*. 2003). Additionally, these studies also indicate that the chlorophyll A/B binding gene *ASCAP9* does not have patterns consistent with significant accelerated rates of evolution in the Hawaiians silversword alliance vs. the progenitor California tarweed lineages (Barrier *et al*. 2001). Nucleotide sequence variation at these loci is used to evaluate levels of genetic differentiation and migration rates between species at each locus, as well as provide evidence for possible different evolutionary histories among loci in the insular adaptive radiation context. The objective of this study is therefore to examine nucleotide sequence diversity and test hypotheses regarding the role of historical demographic factors in shaping patterns of differentiation in these rapidly evolving loci at the population level between two recently derived species of this plant adaptive radiation. The main questions that we address in this study include the following:

1 Does the partitioning of nuclear gene and morphological variation among and within populations and species occur in similar, lineage-specific patterns?

2 Are patterns of genetic diversity and divergence in these species consistent with demographic changes, such as population expansion and gene flow? Does this pattern differ between the duplicated floral regulatory genes sampled and the representative structural housekeeping gene?

3 Do patterns of genetic variation differ between species in the Argyroxiphium lineage (*Argyroxiphium sandwicense*) and members of an active subradiation (*Dubautia arborea* and *D. ciliolata* in the Railliardia clade)?

Materials and methods

Nucleotide sequence data: sample collections and DNA extraction

Leaf tissue samples were collected from approximately 5–10 individuals per population from three populations of *Dubautia arborea* and *Dubautia ciliolata* (Table 1). The three populations sampled from *D. arborea* include individuals from Puu Laau, Puu Mali and a woodland near Waipahoehoe gulch. The three populations sampled from *Dubautia ciliolata* ssp. *glutinosa* include individuals from Puu Kanakaleonui, Puu Kawiiwi and a shrubland near Waipahoehoe gulch (Table 1). The latter taxon is referred to as *D. ciliolata* for the remainder of this study. Leaf tissue samples from 16 plants of *Argyroxiphium sandwicense* ssp. *macrocephalum* were obtained from four localities in Haleakala National Park, Maui: Silversword Loop, Puu o Pele, Ka Moa o Pele, and Puu Naue. This species is referred to as *A. sandwicense* for the remainder of this study. Genomic DNA isolations were extracted from young leaf tissues using a modified rapid plant CTAB (hexadecyltrimethylammonium bromide) protocol (Saghai-Maroof *et al*. 1984). EluQuick (Schleicher and Schuell) glass bead purification was then used on all genomic DNA extractions to reduce the amount of pectin and secondary-product contamination.

Table 1 Nucleotide variation for loci examined in this study

Gene	Species	Length (bp)	n	$n_{locality}$	N_{hap}	S	π_{silent}	θ_π	Tajima's D	Haplotype diversity
ASAP1–A	*A. sandwicense*	1683	15	8/3/1/3	9	21	0.0044	0.0037 (0.0003)	−0.1100	0.886 (0.069)
	D. ciliolata	1661	20	8/6/6	11	27	0.0035	0.0038 (0.0009)	−0.6487	0.900 (0.052)
	D. arborea	1680	20	7/6/7	7	8	0.0016	0.0018 (0.0002)	−1.1372	0.732 (0.092)
ASAP1–B	*A. sandwicense*	1709	15	8/2/2/3	11	18	0.0029	0.0026 (0.0003)	−0.7772	0.952 (0.040)
	D. ciliolata	1736	24	7/12/5	9	13	0.0019	0.0017 (0.0002)	−0.6168	0.880 (0.035)
	D. arborea	1735	19	7/5/7	9	18	0.0021	0.0020 (0.0004)	−1.2315	0.871 (0.051)
ASAP3/TM6–A	*A. sandwicense*	1012	15	8/3/2/2	8	12	0.0036	0.0031 (0.0007)	−0.5782	0.905 (0.046)
	D. ciliolata	949	21	8/8/5	13	22	0.0052	0.0043 (0.0007)	−1.2572*	0.905 (0.047)
	D. arborea	949	18	6/5/7	10	13	0.0030	0.0033 (0.0007)	−0.6855	0.863 (0.064)
ASAP3/TM6–B	*A. sandwicense*	1230	16	8/3/2/3	5	5	0.0014	0.0015 (0.0002)	0.8234	0.683 (0.091)
	D. ciliolata	1247	10	4/4/2	3	2	0.0005	0.0005 (0.0002)	−0.6910	0.511 (0.164)
	D. arborea	1247	1	0/0/1	NA	NA	NA	NA	NA	NA
ASCAB9	*A. sandwicense*	952	15	7/3/2/3	3	3	0.0011	0.0006 (0.0003)	−1.0095	0.448 (0.134)
	D. ciliolata	949	25	8/12/5	15	17	0.0044	0.0033 (0.0004)	−1.0541	0.950 (0.024)
	D. arborea	952	16	7/5/4	10	19	0.0075	0.0057 (0.0005)	−0.1989	0.933 (0.040)

n is the number of individuals/alleles sampled.

$n_{locality}$ is the distribution of individual/allele sampling by locality:
for *Argyroxiphium sandwicense* samples: Silversword Loop/Puu o Pele/Ka moa o Pele/Puu Naue.
for *Dubautia ciliolata* samples: Puu Kanakaleonui/Puu Kawiiwi/Waipahoehoe gulch.
for *Dubautia arborea* samples: Puu Laau/Puu Mali/Waipahoehoe gulch.

S is the number of observed segregating sites.

N_{hap} is the number of haplotypes observed in the given data set, all sites considered.

π_{silent} is nucleotide diversity at silent sites.

θ_π (nucleotide diversity) is the average number of nucleotide differences per site between two sequences, all sites considered.

*significant at the $P < 0.05$ level.

NA (not amplified) refers to lack of *ASAP3/TM6-B* amplification from all but one *D. arborea* individual examined.

PCR amplifications and gene sequencing

To limit misin of incorrect nucleotides, the error-correcting *Pwo* polymerase (Roche) was used in all polymerase chain reaction (PCR) amplifications. An error rate calculation based on multiple amplifications and resequencing of several genes indicates a rate of less that one error in 7–10 kb and no apparent PCR recombinants were present (unpublished observations). Gene-specific amplification primers for *ASAP1*, *ASAP3/TM6*, and *ASCAB9* and amplification of these genes are as previously described (Barrier *et al*. 1999, 2001; Lawton-Rauh *et al*. 2003). Amplified products from these outcrossing, heterozygous individuals were cloned into the pCR-BluntII-TOPO vector using the Zero Blunt TOPO TA cloning kit (Invitrogen) and screened using a restriction-digest approach as described in further detail previously (Lawton-Rauh *et al*. 2003).

All genes were sequenced by primer walking, using ABI 3700 automated DNA sequence analysers (NCSU DNA Sequencing Facility, Iowa State University Sequencing Facility, and NCSU Genome Research Laboratory). Sequences were aligned and edited using the BioLign alignment and editing suite (Tom Hall, 2000–2001) and the CodonCode Phred/Phrap quality index program (CodonCode). All polymorphic sites were confirmed by visual inspection of chromatograms. The DNA sequences are available through GenBank (Accession nos AY259925–AY25993; EU047886–EU047912).

Sequence data analyses

Nucleotide diversity levels were estimated as mean pairwise differences, π (Nei 1987). Estimates of haplotype diversity and nucleotide diversity (θ_π) at all sites and several tests for selection were conducted using the DNASP program version 3.53 (Rozas & Rozas 1999), and assumed that all localities grouped into the same population for each species due to microsatellite data analyses indicating a lack of population structure (Friar *et al*. 2007). The Tajima's *D*-test statistic was used to evaluate deviations from the expectation of the neutral-equilibrium model (Tajima 1989). The significance of Tajima's *D*-test statistics was evaluated via coalescent simulations in DNASP using 10 000 runs, setting the number of segregating sites and the population recombination parameter estimated from the data using SITES (Hey & Wakeley 1997).

Analyses of molecular variance (AMOVA) were conducted to partition molecular variance among species and populations (in this case, localities) using Kimura 2-parameter

distances among haplotypes in ARLEQUIN version 2.0 (Excoffier *et al*. 1992). These analyses were employed in pairwise comparisons between all three species at all loci.

Haplotype networks for each locus were calculated using the 95% statistical parsimony support criterion for inferred gene genealogies (Templeton *et al*. 1992) as implemented in the program TCS version 1.13 (Clement *et al*. 2000). The 95% connection limit was set to the recommended value of 20 inferred missing haplotypes for every network except for *ASAP1-A* and *ASAP1-B*, where the value was set to 23 in order to connect *A. sandwicense* haplotypes to the same network as *D. ciliolata* and *D. arborea*.

The likelihood surfaces for the per gene population-mutation parameter (θ) and population growth rate parameter (g) were jointly estimated and optimized from silent site data using a Markov chain Monte Carlo approach implemented in the program FLUCTUATE (Kuhner *et al*. 1998). Analyses were repeated five times at different chain lengths and step numbers to ensure estimation stability using the following settings: population-mutation parameter estimated from the data (Watterson 1975), search among unconstrained possible exponential growth parameter estimates, randomly inferred genealogy, and starting growth rates of g = 5, 100 and 200 for each initial search. The likelihood ratio test was used to evaluate consistency with population growth expectations ($g > 0$).

The relationship among the estimated parameters of effective population size (N_e), diversity (θ_F), mutation rate per generation (μ), growth rate (g), and time in generations (t) is described by the equation $N_e = (\theta F/2\mu)^{(-g\mu t)}$ (Kuhner *et al*. 1998). To ensure that the joint estimates were not constrained by locus-specific histories (including selection and correlated divergence between homoeologous loci), these parameters were estimated separately at each locus rather than calculated as a converged estimate across loci. The estimated growth rate parameters were used to estimate per-generation population growth rate. This was done by incorporating the mutation rate (μ), which was estimated as an average across all three species employing the equation $\mu = K/2T$ using K(JC) at silent sites with Jukes Cantor correction in DNASP version 3.53 (Nei 1987; Rozas & Rozas 1999).

To examine the relative effects of lineage sorting and migration on haplotype diversity between species, the Bayesian Markov chain Monte Carlo framework of the MDIV program (Nielsen & Wakeley 2001) and IM (Hey & Nielsen 2004) were employed. The MDIV algorithm estimates the joint nonequilibrium values of θ (= $4N_e\mu$), migration rate M (= $2N_em$) and the time to most recent common ancestor [TMRCA = $t/(2N_e)$] between taxa and among all alleles. This procedure was developed to test two alternative hypotheses regarding the divergence between populations or between unstructured species: (i) short divergence times with little migration between taxa vs. (ii) long divergence times with strong migration. The comparison of these alternatives permits testing whether data fit the isolation with subsequent migration model vs. the incomplete isolation with shared ancestral allele model. The IM program is based on the MDIV algorithm and includes additional joint estimates of directional migration between the two taxa examined.

Analyses employing the MDIV and IM algorithms utilized three to eight replicate runs of each pairwise comparison. Each replicate run used different random seeds while optimizing prior maximum value inputs for species divergence time and migration rate both to assess the convergence of estimations and to establish appropriate 95% credibility intervals. MDIV analyses were run using the recommended settings (Nielsen & Wakeley 2001): Hasegawa–Kishino–Yano (HKY) mutation model and 2 million parameter space exploration chains following a burn-in of 50 000 chains. Each IM analysis was run for three preparatory runs for 6 h using different priors followed by parallel runs using similar optimized priors, the HKY mutation model, 6 million burn-in steps, and various random seeds until the estimated sample sizes and curve shapes were optimized. The multilocus runs had the following supplemental settings: five genealogies sampled per chain, two-step heating mode scheme, first heating parameter of 0.05, and second heating parameter of 0.10. The starting prior maximum parameter values differed in each run and the high similarity of posterior distributions indicates that estimates converged to the ergodic average. Additionally, to alleviate the possibility of nonindependence among sites due to significant accelerated rates of nonsynonymous to synonymous evolution (Barrier *et al*. 2001), each locus data set was restricted to silent sites for analyses of population growth rate and migration rates.

Morphological data: measurements and analysis

Six reproductive traits (number of capitula per capitulescence, number of florets per capitulum, receptacular bract length, sepal length, petal length, and ovary length) and two vegetative traits (leaf length and maximum leaf width) were measured to assess the morphological divergence between *D. arborea* and *D. ciliolata* on Mauna Kea. Measurements were recorded from 50 random individuals per population for each species, with three replicate measurements within each individual. The three populations sampled from *D. arborea* and the three populations sampled from *D. ciliolata* are the same populations sampled and assessed for sequence diversity (Table 1).

Analysis of variance (ANOVA) fitting a standard least squares means model with random effects at each level was used to partition the variance in each trait attributable to the following effects: among species, populations within species, and individuals within populations per species, including the variance from replicate measurements within individuals as the error term. All morphological data analyses were conducted using JMP version 4.0.1 (SAS Institute).

Results

Intraspecific genetic variation in regulatory and structural genes

The nucleotide sequences of 15–25 sampled alleles were ascertained for five nuclear genes: *ASAP1-A, ASAP1-B, ASAP3/TM6-A, ASAP3/TM6-B* and *ASCAB9* from *A. sandwicense*, *D. ciliolata*, and *D. arborea*. The exception is *ASAP3/TM6-B* in *D. ciliolata* and *D. arborea*. We were unable to amplify this gene from 14 out of 24 individuals in *D. ciliolata* and from 23 out of 24 individuals in *D. arborea* despite the use of primers that co-amplified this gene with *ASAP3/TM6-A* in all species of the Hawaiian silversword alliance and the North American tarweeds (Barrier *et al*. 1999). These results suggest that a deletion allele for this locus may be present in these two species (Lawton-Rauh *et al*. 2003).

The levels of nucleotide polymorphism and haplotype numbers are shown in Table 1. Estimates of nucleotide diversity (π_{silent}) in all loci in all three species are low, ranging from 0.0005 to 0.0075 (Table 1). The Hudson Kreitman Aguade test (Hudson *et al*. 1987) and the McDonald–Kreitman test of protein evolution (McDonald & Kreitman 1991) [results not shown], as well as the Tajima's test (Table 1) were not significant for all but one gene, suggesting that these loci are evolving according to the neutral-equilibrium model. The exception is *ASAP3/TM6-A* in *D. ciliolata*, which has a polymorphism profile previously found to be consistent with a very recent selective sweep and divergent evolution from its homoeolog *ASAP3/TM6-B* (Lawton-Rauh *et al*. 2003).

Multilocus polymorphism frequency distributions: tests for departures from null demographic and neutral-equilibrium expectations.

The Tajima's *D*-test statistic at silent sites as well as haplotype diversity and nucleotide diversity were estimated for all genes (Table 1). Tajima's *D* reflects the frequency distribution of polymorphisms within a species, and, except for *ASAP3/TM6-B* in *A. sandwicense*, all values of Tajima's *D* are negative. Tajima's *D* for *ASAP3/TM6-A* in *D. ciliolata* is the only negative value that significantly deviates from neutral-equilibrium model expectation. Haplotype diversity estimates indicate the frequency and number of haplotypes and these estimates vary between 0.0 and 1.0. Average nucleotide diversity (θ_π) estimates reflect the average number of pairwise differences per site within a sample and these estimates vary from 0.0000 under no variation to over 0.1000 under very deep divergences among sampled alleles. In all three species, every locus has low nucleotide diversity (ranging from 0.0005 to 0.0057) and high haplotype diversity (ranging from 0.448 to 0.952), a pattern that can occur following population expansion (Grant & Bowen 1998).

The nucleotide diversity at silent sites (θ_F) and growth rate (g) under an exponential population growth model in these three Hawaiian silversword alliance species were jointly estimated using a maximum-likelihood procedure (Kuhner *et al*. 1998). These parameter estimates and the conservative log likelihood ratio test results for the exponential growth vs. no-growth models are shown in Table 2. In *A. sandwicense*, joint estimates in all but one

Table 2 Summary of parameter estimates and test statistics examined for demographic trends. The joint estimate of the parameters θ_F and g in FLUCTUATE (Kuhner *et al*. 1998) followed by the estimated per generation population growth rate based on calculated mutation rates, and the likelihood ratio assessment of deviation from static growth rate. Numbers in parentheses are standard deviations of estimates

Gene	Species	θ_F	g	Per generation	Δln L
ASAP1-A	*A. sandwicense*	0.0076 (0.0019)	461 (214)	7.5×10^{-7}	1.071
	D. ciliolata	0.0048 (0.0011)	148 (149)	2.4×10^{-7}	0.183
	D. arborea	0.0010 (0.0003)	38 (601)	0.6×10^{-7}	0.001
ASAP1-B	*A. sandwicense*	0.0153 (0.0050)	1452 (371)	21.3×10^{-7}	6.489**
	D. ciliolata	0.0047 (0.0010)	2156 (465)	31.7×10^{-7}	4.454**
	D. arborea	0.0083 (0.0024)	1154 (393)	17.0×10^{-7}	3.400**
ASAP3/	*A. sandwicense*	0.0061 (0.0019)	328 (221)	4.1×10^{-7}	0.555
TM6-A	*D. ciliolata*	0.0187 (0.0038)	389 (97)	4.8×10^{-7}	3.081**
	D. arborea	0.0082 (0.0028)	563 (259)	7.0×10^{-7}	1.105
ASAP3/	*A. sandwicense*	0.0003 (0.0001)	−488 (721)	-4.9×10^{-7}	0.098
TM6-B	*D. ciliolata*	0.0016 (0.0010)	10000 (4413)	10.1×10^{-7}	4.139**
	D. arborea	NA	NA	NA	NA
ASCAB9	*A. sandwicense*	0.0030 (0.0009)	3037 (899)	30.7×10^{-7}	3.321
	D. ciliolata	0.0581 (0.0072)	1276 (77)	12.6×10^{-7}	21.929**
	D. arborea	0.0198 (0.0066)	446 (149)	4.5×10^{-7}	2.969**

**$P < 0.01$.

θ_F is the maximum-likelihood estimate of the population-mutation parameter at silent sites jointly estimated with the exponential growth parameter (g).

NA (not amplified) refers to lack of *ASAP3/TM6-B* amplification from all but one *D. arborea* individual.

locus are not significantly different from the static population growth model ($g = 0$). The only exception is *ASAP1-B*, which has a growth rate estimate of $g = \sim 1.5 \times 10^3$. In *D. ciliolata*, four out of five genes examined provide evidence for exponential population expansion, with values of g ranging from ~0.4–10.0 × 10^3. For *D. arborea* genes, the joint estimates can only be calculated for four nuclear genes. Two of these have estimates that are significantly different from expectations of the no-growth model, with significant growth rate parameters of ~1.2 × 10^3 using *ASAP1-B* and ~0.4 × 10^3 using *ASCAB9*.

The pairwise estimates of the time to most recent common ancestor (TMRCA) of alleles (gene divergence) and species (species divergence) are presented in Table 3 as jointly estimated with other parameters using MDIV. Across loci and among pairwise comparisons, estimates of TMRCA among extant alleles are greater than the estimate of time since species divergence in all but one case. The exception is *ASAP3/TM6-B* between *A. sandwicense* and *D. ciliolata* where species divergence is greater than the estimate of allele coalescence (Table 3). There is a notable difference between gene and species coalescence in the comparisons between *D. ciliolata* and *D. arborea*, where species divergence is fairly low (ranging from 0.18 to 0.89) and gene divergence is high and similar to gene divergence estimates between both *Dubautia* species and *A. sandwicense*.

Migration rate (M) and the population-mutation parameter per gene (θ) were jointly estimated and are presented in Table 3. Given the limitations of the MDIV model (Nielsen & Wakeley 2001), we used silent sites in regions of these nuclear genes that did not have evidence of effective recombination (Hey & Nielsen 2004). The silent site, nonrecombining region fragment lengths are indicated in Table 3. Migration rate estimates ($M = 2N_em$) are low between *A. sandwicense* and both *D. ciliolata* and *D. arborea*, with migration rate estimates ranging from 0.01 to 0.15. Nucleotide divergence estimates between *A. sandwicense* and *D. ciliolata* ranged from 1.12 to 5.65 substitutions per gene. Between *A. sandwicense* and *D. arborea*, nucleotide divergence estimates ranged from 1.40 to 7.17 substitutions per gene. It should be noted that these estimates are slightly biased upwards because they are at the very edge of parameter space explored in this algorithm (Nielsen & Wakeley 2001).

In contrast, the inferred migration rates between *D. ciliolata* and *D. arborea* are high, with values ranging from 0.52 to 18.8. These high rate estimates suggest that migration is at a level sufficient to overcome genetic divergence between these two species caused by drift (Griswold & Baker 2002). This notable level of migration was further examined for directionality in both the locus-specific and multilocus contexts using the IM program. These joint estimates were translated into immigration rates in each direction between these two species (M_1 and M_2) and are presented in Table 4. Estimates of M_1 (*D. ciliolata* emigrant alleles into *D. arborea*) in the floral regulatory genes (*ASAP1-A*, *ASAP1-B*, and *ASAP3/TM6-A*) are low and range from 0.0002 to 0.0021 while estimates of M_2 (*D. arborea* emigrant alleles into *D. ciliolata*) are higher and ranged from 0.2636 to an inflated 3228 in *ASAP3/TM6*-A. In contrast, in the structural locus (*ASCAB9*) estimates of M_1 and M_2 are high (Table 4). This suggests that alleles are migrating in both directions in the structural locus and in only one direction in all three regulatory loci. The extent of this directionality is shown as a ratio of M_2/M_1 (Table 4).

Table 3 MDIV (Nielsen & Wakeley 2001) joint estimates of gene and species divergence times ($T = t/2N_e$), migration rate ($M = 2N_em$), and the population mutation parameter ($\theta = 4N'_e$); 95% credibility intervals are indicated in parentheses. 'Length of segment' refers to the length (bp) of each nonrecombining region (silent sites only) used for each locus in MDIV analyses

	Locus	Length of segment (bp)	Gene divergence	Species divergence	Migration rate (M)	θ
D. ciliolata vs.	ASAP1-A	607	3.21	0.42 (0.18, 9.50)	0.52 (0.02, 2.40)	1.72 (0.86, 3.47)
D. arborea	ASAP1-B	1502	1.79	0.89 (0.18, 4.81)	0.87 (0.1, 3.24)	3.44 (2.00, 6.52)
	ASAP3/TM6-A	440	3.69	0.18 (0.04, 19.00)	18.8 (2.76, 20.00)	2.03 (0.87, 3.64)
	ASCAB9	309	3.40	0.65 (0.24, 11.59)	8.13 (2.46, 14.91)	1.30 (0.59, 2.86)
A. sandwicense vs.	ASAP1-A	606	3.76	2.81 (1.15, 6.92)	0.01 (0.01, 0.39)	4.77 (2.75, 8.54)
D. ciliolata	ASAP1-B	1472	4.21	2.66 (1.30, 9.92)	0.02 (0.01, 0.41)	5.65 (2.80, 9.31)
	ASAP3/TM6-A	435	3.00	1.56 (0.68, 9.52)	0.04 (0.01, 0.57)	2.72 (1.40, 5.42)
	ASAP3/TM6-B	1083	9.36	10.53 (2.91, 15.00)	0.01 (0.01, 0.33)	1.12 (0.47, 2.44)
	ASCAB9	332	3.24	1.96 (0.56, 9.54)	0.15 (0.03, 0.93)	1.12 (0.43, 2.58)
A. sandwicense vs.	ASAP1-A	619	5.83	4.42 (1.64, 9.86)	0.01 (0.01, 0.34)	2.88 (1.57, 5.42)
D. arborea	ASAP1-B	1472	3.40	2.25 (0.91, 4.88)	0.01 (0.01, 0.40)	7.17 (4.45, 12.22)
	ASAP3/TM6-A	435	4.20	2.94 (1.14, 9.68)	0.01 (0.01, 0.42)	1.40 (0.57, 3.01)
	ASCAB9	333	3.30	2.14 (0.56, 9.52)	0.02 (0.01, 0.81)	1.56 (0.70, 3.65)

Table 4 IM joint estimates of the population mutation parameter ($\theta = 4N_e\mu$), migration rate ($m = m/\mu$), divergence times ($T = t/2N_e$), and subsequent ratios among these parameters. The '1' notation refers to *Dubautia arborea*, '2' refers to *Dubautia ciliolata*, and 'A' refers to the common ancestor joint estimates. The 95% credibility intervals for the posterior distributions of the estimated parameters are indicated in parentheses. θ_2/θ_1, θ_A/θ_1 and θ_A/θ_2 reflect relative population sizes of the representative compared lineages. M_1 and M_2 are the population migration rate estimates [i.e. $M_1 = 2N_1m_1 = (m_1 * \theta_1)/2$]. M_2/M_1 reflect relative population migration rates between *D. arborea* and *D. ciliolata*

	ASAP1A	ASAP1B	ASAP3A	ASCAB9	Multilocus
θ_1	0.010 (0.023, 2.055)	0.031 (0.0306, 1.742)	0.844 (0.282, 3.792)	1.742 (0.799, 16.382)	1.026 (0.457, 2.892)
θ_2	3.400 (1.566, 13.623)	3.515 (1.681, 50.154)	1141.583 (55.465, 1615.104)	2.130 (1.015, 5.485)	2.686 (1.566, 5.681)
θ_A	0.925 (0.3438, 14.861)	1.987 (1.070, 59.445)	3.990 (0.811, 32.269)	0.008 (0.412, 16.399)	1.890 (0.221, 9.521)
m_1	0.005 (0.095, 9.515)	0.010 (0.170, 19.150)	0.005 (0.115, 9.505)	15.775 (4.825, 48.725)	1.515 (0.185, 8.755)
m_2	0.205 (0.055, 4.995)	0.150 (0.070, 7.030)	5.655 (3.045, 27.615)	0.021 (0.024, 0.974)	0.205 (0.055, 5.325)
t	4.450 (0.710, 19.470)	5.315 (1.135, 9.795)	4.950 (4.150, 97.650)	13.025 (2.875, 48.725)	1.750 (0.730, 19.450)
θ_2/θ_1	34.24	114.86	1352.59	1.22	2.62
θ_A/θ_1	9.31	64.92	4.73	0.00	1.84
θ_A/θ_2	0.27	0.57	0.003	0.00	0.70
M_1	0.0002	0.0003	0.0021	13.7380	0.7773
M_2	0.3490	0.2636	3228	0.2180	0.2753
M_2/M_1	1407.3	861.4	1537000	0.002	0.35

Table 5 AMOVA and fixation indices for loci examined in this study: *Argyroxiphium sandwicense* vs. *Dubautia arborea* (*D. arb*) and *Dubautia ciliolata* (*D. cilio*)

	ASAP1–A		*ASAP1–B*		*ASAP3/TM6–A*		*ASAP3/TM6–B*		*ASCAB9*	
Source of variation (%)	*D. arb*	*D. cilio*	*D. arb*	*D. cilio*	*D. arb*	*D. cilio*	*D. arb*	*D. cilio*	*D. arb*	*D. cilio*
Among species	83.24	74.05	78.03	79.52	61.78	43.45	NA	85.43	56.23	55.27
Among populations within species*	0.71	−0.40	−0.97	−1.29	2.36	−1.08	NA	3.35	3.00	10.23
Within populations	16.05	26.36	22.94	21.77	35.86	57.63	NA	11.22	40.76	34.50
Fixation indices										
Φ_{CT} (species total)	0.832	0.740	0.780	0.795	0.618	0.434	NA	0.854	0.562	0.553
Φ_{SC} (population/species)*	0.042	−0.016	−0.044	−0.063	0.062	−0.019	NA	0.230	0.069	0.229
Φ_{ST} (population/total)	0.839	0.736	0.771	0.782	0.641	0.424	NA	0.888	0.592	0.655

NA (not amplified) refers to lack of *ASAP3/TM6-B* amplification from all but one *D. arborea* individual.
*Negative variance measures and fixation indices occur because these values are neither covariances nor correlation coefficients, respectively, and indicate lack of within-species genetic structure.

Partitioning of molecular covariances and haplotype distributions among populations and species in regulatory and structural genes

Analysis of molecular covariance (AMOVA) was used to partition haplotype diversity for these loci into among-species, among-population (locality), and within-population (locality) variation (Excoffier *et al*. 1992). AMOVA comparisons between *A. sandwicense* and both *D. ciliolata* and *D. arborea* indicate that most molecular variation is due to among-species divergence in the five nuclear genes in this study (Table 5). The only exception is the *ASAP3/TM6-A* gene between *A. sandwicense* and *D. ciliolata*, where most variation occurs at the intrapopulation level; among-species variation accounts for 43.5% of total haplotype variation at this locus.

The fixation index (Φ) estimates the correlation of haplotypes within a subgroup drawn from the entire group and is calculated using the above AMOVA covariance components. The correlation of interspecific haplotypes drawn from both species is Φ_{CT}, interpopulation haplotypes drawn within a species is Φ_{SC}, and interpopulation haplotypes drawn from both species is Φ_{ST} (Excoffier *et al*. 1992). The Φ_{CT} and Φ_{ST} molecular fixation indices are high for all genes in comparisons between *A. sandwicense* and either *D. arborea* or *D. ciliolata* (see Table 5). The levels of Φ_{CT} between *A. sandwicense* and *D. ciliolata* ranged from 0.434 to 0.854, while Φ_{CT} estimates between *A. sandwicense* and *D. arborea* ranged from 0.562 to 0.832.

For the comparisons between *D. ciliolata* and *D. arborea*, most molecular variation is found within species, with approximately 80% of the haplotype variation occurring within populations (see Table 6). The interpopulation-total fixation indices (Φ_{ST}) are higher than the interspecific-total indices (Φ_{CT}) and the interpopulation-species indices (Φ_{SC})

Table 6 AMOVA and fixation indices for loci examined in this study: *Dubautia arborea* vs. *Dubautia ciliolata*

Source of variation (%)	*ASAP1-A*	*ASAP1-B*	*ASAP3/TM6-A*	*ASCAB9*
Among species	18.61	16.74	16.66	4.11
Among populations within species*	1.27	6.26	−5.03	6.45
Within populations	80.13	77.00	88.37	89.44
Fixation indices				
Φ_{CT} (species/total)	0.186	0.167	0.167	0.041
Φ_{SC} (population/species)*	0.016	0.075	−0.060	0.067
Φ_{ST} (population/total)	0.199	0.230	0.116	0.106

*Negative variance measures and fixation indices occur because these values are neither covariances nor correlation coefficients, respectively, and indicate lack of within-species genetic structure.

in *ASAP1-A*, *ASAP1-B*, and *ASCAB9*. The interpopulation-total fixation index (Φ_{ST}) is notably high in *ASAP1-A* and *ASAP1-B* at 0.199 and 0.230, respectively. There are moderate levels of Φ_{CT} in *ASAP1-A*, *ASAP1-B*, and *ASAP3/TM6-A* (0.167–0.186) with estimates at least fourfold higher than the value estimated in *ASCAB9* (0.041). The interpopulation-species fixation index (Φ_{SC}), which estimates between-population differentiation within species (as opposed to Φ_{ST}, which estimates differentiation across all populations regardless of species) is low in all four genes, ranging from 0.016 in *ASAP1-A* to 0.075 in *ASAP1-B*.

The inferred haplotype networks for all five nuclear genes are shown in Fig. 2. All inferred nuclear gene haplotype networks indicate separate clades with no shared haplotypes between *A. sandwicense* and either *Dubautia* species. In contrast, there is significant haplotype sharing between the sibling species *D. ciliolata* and *D. arborea* for all nuclear genes except *ASAP1-A* (see Fig. 2A–E). Additionally, the inferred haplotype networks for *ASAP3/TM6-A* and *ASCAB9* indicate evidence of homoplasy between two haplotypes (see Fig. 2C–E). This homoplasy is probably due to recombination and is consistent with the moderate level of estimated recombination in these two genes (results not shown).

Morphological variance partitioning among populations and between D. arborea *and* D. ciliolata

The extent of morphological divergence between two closely related species can be measured to examine how the variance of particular phenotypes is partitioned across hierarchies of population structure as well as to support taxonomic divisions among species. Eight morphological traits (six reproductive and two vegetative) were analysed between the sibling species *D. ciliolata* and *D. arborea* to determine the pattern of phenotypic variance across hierarchies of population structure and to compare this pattern to molecular differentiation at multiple loci.

Quantitative measures of these eight morphological features are shown on Table 7. Nested analysis of variance (ANOVA) indicates that a significant amount of the quantitative variation in morphology is attributable to differences among populations and individuals within populations ($P < 0.001$, Table 8). A substantial proportion of the morphological variation is due to among-species differentiation for two out of the six reproductive traits examined [number of capitula per capitulescence ($R^2 = 74.0\%$) and number of florets per capitulum ($R^2 = 63.6\%$)] and in both vegetative traits [leaf length ($R^2 = 83.1\%$) and maximum leaf width ($R^2 = 83.9\%$)]. The differences among species for these traits are significant ($P < 0.01$). It should be noted that because the morphological measurements used in these analyses were not conducted under common garden conditions (they were measured in the field), we cannot directly partition the variances attributable to genetic and environmental components. Analyses of these data can, however, evaluate the phenotypes used to taxonomically

Table 7 Morphological trait analyses in *Dubautia ciliolata* and *Dubautia arborea*. Morphological trait means with 95% confidence intervals (CI) and standard errors (SE). All measurements are in millimetres

Trait	Species	Trait mean (CI)	SE
No. of capitula/ capitulescence	*D. ciliolata*	3.120 (2.73, 3.51)	0.079
	D. arborea	15.682 (15.29, 16.07)	0.235
No. of florets/ capitulum	*D. ciliolata*	8.646 (8.08, 9.21)	0.108
	D. arborea	22.704 (22.14, 23.27)	0.341
Receptacular bract length	*D. ciliolata*	8.039 (7.90, 8.18)	0.055
	D. arborea	8.860 (8.72, 9.00)	0.068
Sepal length	*D. ciliolata*	5.147 (5.07, 5.23)	0.032
	D. arborea	4.389 (4.31, 4.47)	0.040
Corolla length	*D. ciliolata*	5.412 (5.33, 5.49)	0.031
	D. arborea	6.532 (6.45, 6.61)	0.039
Ovary length	*D. ciliolata*	4.407 (4.33, 4.48)	0.029
	D. arborea	4.836 (4.76, 4.91)	0.037
Leaf length	*D. ciliolata*	14.190 (13.4, 15.0)	0.159
	D. arborea	47.750 (46.9, 48.6)	0.479
Maximum leaf width	*D. ciliolata*	2.940 (2.69, 3.19)	0.029
	D. arborea	13.600 (13.35, 13.85)	0.153

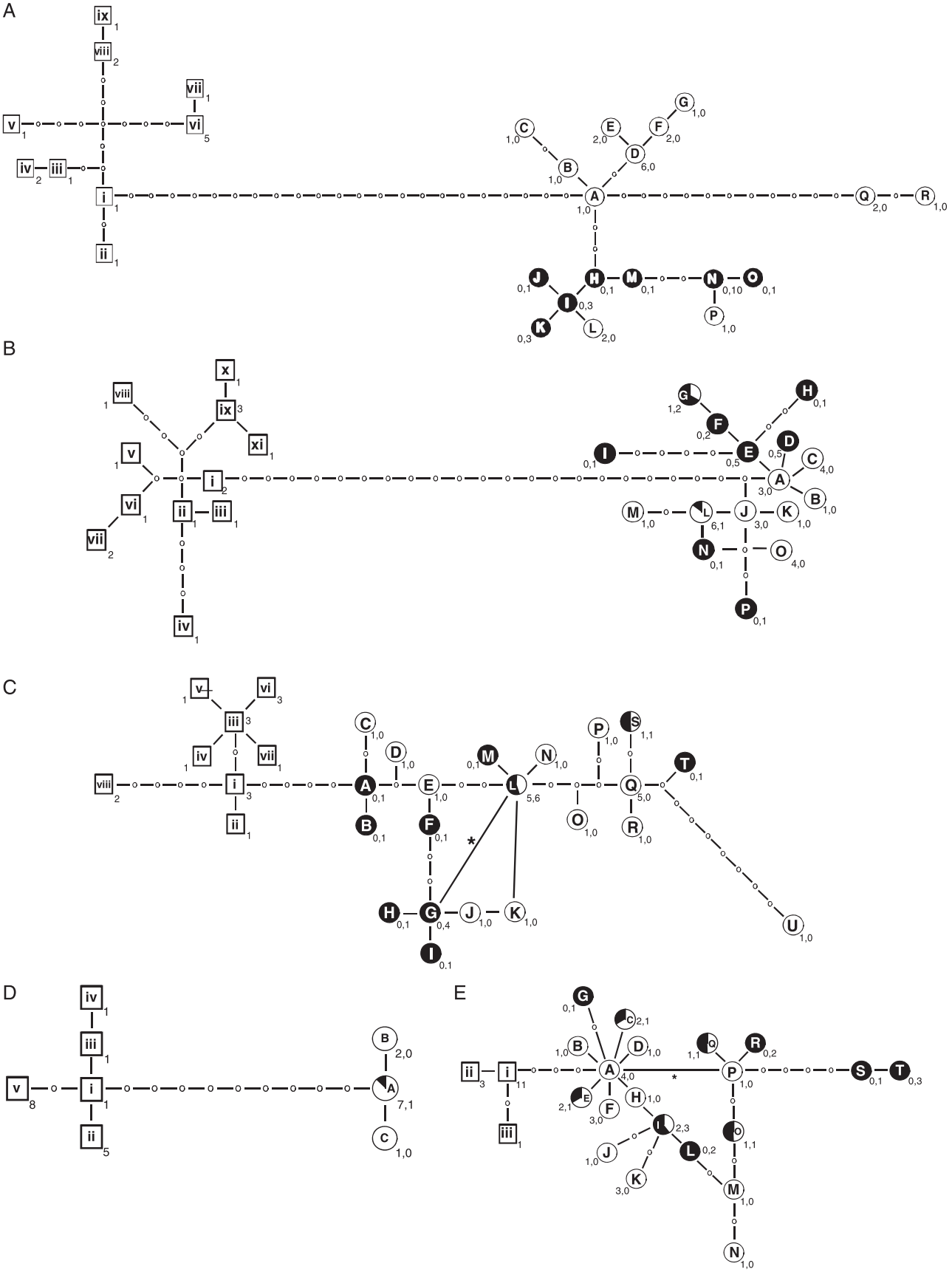

Table 8 ANOVA of morphological traits in *Dubautia ciliolata* and *Dubautia arborea*. VarComp values are estimates of variance components for each random effect level of variation, with the total model variance in parentheses; % total values are the percentages of each component out of the total model variance in the VarComp column

Trait	Source of variation	DF	MS	*F* ratio	Prob > *F*	R^2	VarComp	% total
No. of capitula/ capitulescence	Species	1	35170.1	192.2	0.0002	0.740	78.40	84.82
	Populations within species	4	183.0	6.8	< 0.0001	0.015	1.05	1.14
	Individuals within population per species	294	26.91	4.5	< 0.0001	0.167	7.02	7.60
	Error	595	5.96			0.075	5.96 (92.4)	6.45
No. of florets/ capitulum	Species	1	44343	23.2	0.0086	0.636	95.05	74.38
	Populations within species	4	1922.0	47.7	< 0.0001	0.110	12.65	8.90
	Individuals within population per species	294	40.4	4.1	< 0.0001	0.170	10.24	8.02
	Error	595	9.9			0.084	9.85 (127.8)	7.71
Receptacular bract length	Species	1	151.1	4.3	0.1065	0.089	0.26	12.61
	Populations within species	4	35.1	9.7	< 0.0001	0.083	0.21	10.25
	Individuals within population per species	294	3.6	6.5	< 0.0001	0.632	1.03	49.99
	Error	595	0.6			0.197	0.56 (2.06)	27.15
Sepal length	Species	1	127.5	4.2	0.1096	0.193	0.22	24.79
	Populations within species	4	30.3	32.3	< 0.0001	0.184	0.20	22.50
	Individuals within population per species	294	0.9	4.3	< 0.0001	0.418	0.24	27.25
	Error	595	0.2			0.202	0.22 (0.88)	25.47
Corolla length	Species	1	280.3	21.5	0.0098	0.365	0.60	51.06
	Populations within species	4	13.0	13.3	< 0.0001	0.068	0.08	6.91
	Individuals within population per species	294	1.0	4.0	< 0.0001	0.375	0.25	20.96
	Error	595	0.3			0.188	0.25 (1.17)	21.07
Ovary length	Species	1	41.8	6.7	0.0615	0.086	0.08	13.48
	Populations within species	4	6.3	6.6	< 0.0001	0.052	0.04	6.08
	Individuals within population per species	294	1.0	4.0	< 0.0001	0.575	0.24	40.57
	Error	595	0.2			0.288	0.24 (0.59)	39.86
Leaf length	Species	1	253506	130.5	0.0003	0.831	559.03	90.07
	Populations within species	4	1943.2	16.5	< 0.001	0.026	12.17	1.96
	Individuals within population per species	294	117.6	7.6	< 0.001	0.113	34.06	5.49
	Error	600	15.4			0.030	15.39 (620.6)	2.48
Maximum leaf width	Species	1	25569.1	182.4	0.0002	0.839	56.51	90.72
	Populations within species	4	140.2	12.1	< 0.001	0.018	0.86	1.38
	Individuals within population per species	294	11.6	7.2	< 0.001	0.111	3.32	5.32
	Error	600	1.6			0.032	1.61 (62.29)	2.58

distinguish these two closely related species and to examine the relative partitioning of natural trait variation manifested in the field environment.

Discussion

Adaptive radiation, especially among insular species, occurs through a dynamic series of ecological interactions across changing environmental gradients. Examining population demographic models of adaptive radiations can therefore be complex and difficult to separate from the effects of natural selection, especially without extensive genome-wide data. For this reason, the evolutionary forces shaping nucleotide sequence divergence in adaptive radiations has primarily been assumed rather than empirically investigated (Schluter 2000). Molecular population genetic analyses, however, can allow us to infer the influences of factors such as genetic differentiation, population expansion,

Fig. 2 Statistical parsimony haplotype networks of all genes examined in this study from *Argyroxiphium sandwicense*, *Dubautia arborea*, and *Dubautia ciliolata*. (A) *ASAP1-A*, (B) *ASAP1-B*, (C) *ASAP3/TM6-A*, (D) *ASAP3/TM6-B*, (E) *ASCAB9*. Squares indicate *A. sandwicense* haplotypes (labelled in lowercase roman numerals) with the number of sampled individuals of each haplotype denoted by subscripted numbers. Circles indicate *D. ciliolata* and *D. arborea* haplotypes (labelled in uppercase letters) with *D. ciliolata* haplotypes depicted as white circles and *D. arborea* haplotypes depicted as black circles. Shared haplotypes between *D. ciliolata* and *D. arborea* are denoted as pie charts. The first subscript number below *Dubautia* haplotypes denotes the number of *D. ciliolata* sampled individuals with the designated haplotype and the second subscript number denotes the number of *D. arborea* individuals with the same haplotype.
*indicates homoplasy between haplotypes G and L in *ASAPETALA3/TM6-A*. Haplotype labels are cross-referenced with haplotype sequences shown in the Appendix.

and migration (hence, allele-sharing) in adaptive radiations and thus shed some light regarding the relative role of stochastic and deterministic forces (Wright 1955; Gillespie 2001). We compared the patterns of variance partitioning between the nuclear loci investigated and several morphological features between two recently derived species. Using a multilocus approach, we investigated the relative contributions of isolation and migration as well as the patterns of historical population size change among multiple loci across three Hawaiian silversword alliance species.

Genetic variation and signatures of population expansion in the Hawaiian silversword alliance

The patterns of nucleotide polymorphisms across five nuclear genes suggest the hypothesis that all three species have undergone recent population expansion. The negative values of Tajima's *D* (see Table 1) indicate an excess of low frequency polymorphisms within species, and the consistently negative value of *D* across the multiple genes in these species can be interpreted as evidence for historical population expansion (Tajima 1989). This hypothesis of population expansion is also supported by examining the relative levels of nucleotide and haplotype diversity (Grant & Bowen 1998). For all genes within each species, haplotype diversity estimates are high and nucleotide diversity estimates are low (see Table 1), a pattern associated with recent population expansion (Grant & Bowen 1998).

Further analyses suggest that this expansion is consistent with an exponential growth model in *D. ciliolata*, even after Bonferonni correction for multiple testing (results not shown). The pattern of nucleotide polymorphisms in one out of five loci in *A. sandwicense*, four out of five loci in *D. ciliolata* and two out of four in *D. arborea* rejects a no-growth model in favour of an exponential growth model under an estimated growth parameter ($P < 0.01$, Table 2). In contrast to *D. ciliolata*, these results in *D. arborea* and *A. sandwicense* are mixed, possibly reflecting population expansion histories that do not follow the dramatic exponential model. All three species have experienced recent human-mediated population decline with the last 200 years. Thus, the levels and patterns of observed nucleotide polymorphisms in these species represent the effects of events that occurred prior to this decline (and subsequent recovery) (see also Friar *et al*. 2001). Furthermore, comparison of estimated population sizes between each *Dubautia* species vs. their most recent common ancestor (reflected in θ_A/θ_1 vs. θ_A/θ_2 in Table 4) suggests that population expansion occurred at a higher rate in *D. ciliolata* than in *D. arborea*. This population expansion may be associated with the colonization of new ecological niches that presumably arise from the dynamic geology of the Hawaiian archipelago (Carson & Clague 1995). The difference in rates of population expansion between *D. arborea* and *D. ciliolata* suggests that these taxa were subjected to contrasting colonization restrictions, perhaps through different ecological vulnerabilities or lineage divergence times.

Variance partitioning in nuclear loci and morphological traits within and between recently diverged species

The three taxa used in this study represent species that have diverged both relatively early and recently from each other in this adaptive radiation. *Argyroxiphium sandwicense* last shared a common ancestor with the two *Dubautia* species approximately 5.2 Ma (Baldwin & Sanderson 1998). *D. ciliolata* and *D. arborea* are species that appear to be among the most recently derived species of the Hawaiian silversword alliance and both are endemic to Hawaii, the youngest island of the Hawaiian archipelago (Baldwin & Robichaux 1995). This island emerged approximately 0.5 Ma, suggesting a very recent origin of these species (MacDonald *et al*. 1983; Carr 1985; Witter & Carr 1988; Carson & Clague 1995; Baldwin & Sanderson 1998). Moreover, there is at least one hybrid zone on Mauna Kea containing what appear to be members of both species and early generation hybrids between these species (Remington & Robichaux 2007).

Remarkably high levels of morphological differentiation (Carr 1985; Robichaux *et al*. 1990) and low levels of genetic differentiation (Witter & Carr 1988) characterize the Hawaiian silversword alliance. Our morphological analyses of six reproductive traits and two vegetative traits show that the rapid morphological divergence characterizing the Hawaiian silversword alliance adaptive radiation is significant, even between the recently diverged *Dubautia* species. Analysis of variance (ANOVA) for each trait between the sibling species *D. ciliolata* and *D. arborea* indicates significant quantitative divergence in five of these morphological traits (see Tables 7 and 8). Interestingly, morphological trait variance partitioning follows the same general pattern found in the regulatory gene AMOVA calculations in Table 6. The regulatory loci in this study also have higher fixation indices occurring among species vs. total (Φ_{CT}) compared to the structural gene. This fixation index in the structural gene is similar to indices estimated based on AFLP and allozyme loci (Witter & Carr 1988; Remington & Robichaux 2007), suggesting that the duplicated regulatory loci in this study may have a pattern that differs from other loci. We hope to test this hypothesis using a significantly larger multilocus data set containing more nuclear genes of different functions.

Significant morphological differentiation between *D. arborea* and *D. ciliolata* is observed despite low levels of genetic differentiation. Analyses of neutral markers including allozymes (Nei's genetic distance = 0.058; Witter & Carr 1988), microsatellites (Friar *et al*. 2007), and AFLP markers ($F_{ST} = 0.086$; Remington & Robichaux 2007) indicate that *D. ciliolata* and *D. arborea* are not strongly differentiated at

the genetic level. Our molecular population genetic analyses of gene-encoding nuclear loci reinforce these studies. AMOVA assessing covariation in the four loci examined in this study, however, provides mixed results. Species differentiation (Φ_{CT}) between these two sibling species is low in the structural housekeeping gene *ASCAB9* but is moderate in the three floral regulatory genes (*ASAP1-A*, *ASAP1-B*, and *ASAP3/TM6-A*) [see Table 6].

The moderate levels of Φ_{CT} between these two species occur despite the lack of fixed differences and the presence of shared haplotypes in most nuclear genes, resulting in a lack of reciprocal monophyly in the haplotype networks. While there are no fixed molecular differences between *D. ciliolata* and *D. arborea*, haplotype networks indicate several species-specific haplotypes (see Fig. 2) as well as differences in the frequencies of shared haplotypes within each species; together, these contribute to the observed levels of nucleotide differentiation between *D. ciliolata* and *D. arborea*. Thus, although previous allozyme and AFLP studies indicate that overall genetic divergence between these two species is low, the distributions of haplotypes suggest a greater degree of nucleotide sequence differentiation in these loci between the sibling species in this study.

Gene flow within the adaptive radiation

Gene flow (i.e. allele migration), by contributing to allele exchange, has been hypothesized to impede or prevent species differentiation (Mayr 1942). Paradoxically, however, it has also been suggested that, in some cases, it may actually promote divergence between lineages (Caisse & Antonovics 1978; Church & Taylor 2002; Rieseberg *et al*. 2004). Migration between incipient species has been documented in several cases, including sympatric smelt (Saint-Laurent *et al*. 2003), African cichlids (Hey *et al*. 2004), and sunflowers (Rieseberg *et al*. 2004), suggesting that gene flow can occur during the speciation process. Our results here further suggest that despite clear phenotypic differentiation between members of the Hawaiian silversword alliance, the impact of gene flow is still observed at the molecular level between recently diverged species and that this may occur through differential allele-sharing among loci (Table 4).

Migration rates between the two distantly related groups (*A. sandwicense* and the two *Dubautia* species) are negligible and are at the limit of parameter space in this MDIV analysis (Table 3). In contrast, migration rates are fairly high between the two *Dubautia* species, which may account for at least some fraction of the observed shared haplotypes for nuclear genes (Fig. 2). Furthermore, the direction of allele-sharing between *D. arborea* and *D. ciliolata* occurs in different directions between the floral regulatory loci studied (*ASAP1-A*, *ASAP1-B*, and *ASAP3-A*) and the structural locus studied (*ASCAB9*; see Table 4). For the floral regulatory loci, there are essentially no alleles migrating from *D. ciliolata* to *D. arborea* (no immigrant alleles in *D. arborea*, indicated in the low range of M_1 from 0.0002 to 0.0021), yet alleles move at a moderate-to-high rate from *D. arborea* to *D. ciliolata* (M_2 ranges from 0.2636 to 3228). The opposite is true for the structural locus: allele migration is apparent in both directions, with a much larger number of alleles migrating from *D. ciliolata* to *D. arborea* ($M_2/M_1 = 0.002$).

Allele movement between these two species is not surprising. *D. ciliolata* and *D. arborea* are interfertile and their species ranges overlap on Mauna Kea. Additionally, at least one hybrid zone between these two species is known (Carr & Kyhos 1981), which indicates that hybridization between the two species can occur and may serve as the basis for historical and current gene flow. It is not uncommon for divergent taxa to share alleles following lineage separation (Hey *et al*. 2004). Recent studies of sympatric host races of the larch budmoth even suggest that selection-driven genetic divergence during ecological speciation can coincide with gene flow and may even be a common feature of the speciation process (Emelianov *et al*. 2003).

Our results of gene flow directionality suggest that speciation in the Hawaiian silversword adaptive radiation may coincide with differential gene flow resulting in alleles at some loci being shared differently than alleles at other loci. Divergent selection during adaptive differentiation accompanied by high rates of allele-sharing among sympatric taxa has also been documented in a recent study of sympatric smelt (Saint-Laurent *et al*. 2003). The latter study indicates that gene flow has not prevented a directional effect of selection on phenotypic divergence between two smelt ecotypes (Saint-Laurent *et al*. 2003).

In the context of the differentiation between *D. ciliolata* and *D. arborea*, gene flow may moderate the extent of adaptive divergence between species, but divergent selection appears to have been strong enough to maintain phenotypic differentiation despite high rates of migration. Additionally, our analyses of floral regulatory loci and a structural locus indicate that mechanisms may exist to partition allele-sharing among loci of different function. To our knowledge, our results indicating alternative directions of allele-sharing across loci, especially of presumably different gene classes, are the first of their kind and present an exciting hypothesis regarding the historical molecular population genetic mechanisms underlying adaptive diversification. We hope to test this hypothesis, and related extensions of this hypothesis, using future, more exhaustive multilocus sampling.

One extended hypothesis for the mechanism responsible for the observed differential rate of allele-sharing between the regulatory loci and the structural locus is that the high outcrossing rate exhibited in most Hawaiian silversword alliance species (Friar *et al*. 2007) may result in an increased rate of effective recombination (Wright *et al*. 2002), thus permitting the partitioning of locus-specific differences in

allele migration and allowing alternative directions of allele-sharing among different loci. These differences in rates of effective recombination could therefore lead to differences in potential allele exchange through the process described as 'genetic draft' (Gillespie 2001), leading to 'mosaic' genomic differentiation between diverging species (Wu 2001). Perhaps, it is through such alternative rates of allele exchange among lineages that certain loci of larger phenotypic effect can become locally adaptive and even lead to the accelerated rate of speciation associated with adaptive radiations. This is particularly interesting in light of contrasting patterns of molecular covariance partitioning and allele-sharing in the floral regulatory genes vs. the structural gene, microsatellite markers (Friar *et al.* 2007), and AFLP markers (Remington & Robichaux 2007). The differences in variance partitioning and allele movement of floral regulatory genes between species, when considered in the background of high outcrossing and moderate recombination rates, suggest that these loci (or linked loci) could be under positive selection in *D. ciliolata* or under weak purifying selection in *D. arborea*. If these loci are under positive selection in *D. ciliolata*, then allele-sharing between these two species may be a mechanism increasing allele frequency in *D. ciliolata* more quickly than if the two species were completely isolated from each other. This would be an example of collective evolution, where moderate levels of gene flow between species may actually accelerate divergence of lineages (Morjan & Rieseberg 2004). Alternatively, if these loci are under weak purifying selection in *D. arborea*, then allele-sharing between these two species may simply prevent total loss of the alleles under purifying selection. Future among- and within-population studies utilizing multiple loci representing greater portions of the genome will be necessary to address the hypotheses presented above.

Acknowledgements

The authors thank E. Friar, J. Hey, T.F.C .Mackay, B. Rauh, D. Remington and members of both the Purugganan Laboratory and the Mitchell-Olds Laboratory for insightful discussions. M. Barrier, E. Friar, S. Halldorsdottir and D.L. Remington assisted with field measurements of *Dubautia arborea* and *D. ciliolata* morphologies. Leaf tissue samples from *Argyroxiphium sandwicense* ssp. *macrocephalum* from Puu o Pele, Ka moa o Pele, and Puu Naue localities were kindly provided by E. Friar. The Clemson University Genome Institute (CUGI) and the Max Planck Institute for Chemical Ecology provided supplemental computer resources and time. This work is supported by a grant from the National Science Foundation (to M.D.P. and R.H.R.), an Alfred P. Sloan Foundation Young Investigator Award (to M.D.P.), a Sigma Xi Grant in Aid of Research Award (to A.L.R.), and Clemson University.

References

Baldwin BG (1997) Adaptive radiation of the Hawaiian silversword alliance: congruence and conflict of phylogenetic evidence from molecular and non-molecular investigations. In: *Molecular Evolution and Adaptive Radiation* (eds Givnish TJ, Sytsma KJ), pp. 103–128. Cambridge University Press, Cambridge, UK.

Baldwin BG, Robichaux R (1995) Historical biogeography and ecology of the Hawaiian silversword alliance: new molecular phylogenetic perspectives. In: *Hawaiian Biogeography: Evolution on a Hot Spot Archipelago* (eds Wagner WL, Funk VA), pp. 259–287. Smithsonian Institution Press, Washington, D.C.

Baldwin BG, Kyhos DW, Dvorak J, Carr GD (1991) Chloroplast DNA evidence for the North American origin of the Hawaiian silversword alliance (Asteraceae). *Proceedings of the National Academy of Sciences, USA*, **88**, 1840–1843.

Baldwin BG, Sanderson M (1998) Age and rate of diversification of the Hawaiian silversword alliance (Compositae). *Proceedings of the National Academy of Sciences, USA*, **95**, 9402–9406.

Baldwin BG, Wessa BL (2000) Origin and relationships of the tarweed-silversword lineage (Compositae-Madiinae). *American Journal of Botany*, **87**, 1890–1908.

Barrier M, Baldwin BG, Robichaux RH, Purugganan MD (1999) Interspecific hybrid ancestry of a plant adaptive radiation: allopolyploidy of the Hawaiian silversword alliance (Asteraceae) inferred from floral homoeotic gene duplications. *Molecular Biology and Evolution*, **16** (8), 1105–1113.

Barrier M, Robichaux RH, Purugganan MD (2001) Accelerated regulatory gene evolution in an adaptive radiation. *Proceedings of the Nature Academy of Sciences of the USA*, **98** (18), 10208–10213.

Beerli P, Felsenstein J (1999) Maximum-likelihood estimation of migration rates and effective population numbers in two populations using a coalescent approach. *Genetics*, **152**, 763–773.

Bulgin NL, Gibbs HL, Vickery P, Baker AJ (2003) Ancestral polymorphisms in genetic markers obscure detection of evolutionarily distinct populations in the endangered Florida grasshopper sparrow (*Ammodramus savannarum floridanus*). *Molecular Ecology*, **12**, 831–844.

Caisse M, Antonovics J (1978) Evolution in closely adjacent plant populations. IX. Evolution of reproductive isolation in clinal populations. *Heredity*, **40**, 371–384.

Carr GD (1978) Chromosome numbers of Hawaiian flowering plants and the significance of cytology in selected taxa. *American Journal of Botany*, **65**, 236–242.

Carr GD (1985) Monograph of the Hawaiian Madiinae (Asteraceae): *Argyroxiphium, Dubautia,* and *Wilkesia*. *Allertonia*, **4**, 1–123.

Carr GD, Kyhos DW (1981) Adaptive radiation in the Hawaiian silversword alliance (Compositae-Madiinae). I. Cytogenetics of spontaneous hybrids. *Evolution*, **35**, 543–556.

Carson HL, Clague DA (1995) Geology and Biogeography of the Hawaiian Islands. In: *Hawaiian Biogeography: Evolution on a Hot Spot Archipelago* (eds Wagner WL, Funk VA), pp. 14–29. Smithsonian Institution Press, Washington, D.C.

Chase VC, Raven PH (1975) Evolutionary and ecological relationships between *Aquilegia formosa and A. pubescens* (Ranunculaceae), two perennial plants. *Evolution*, **29**, 474–486.

Church SA, Taylor DR (2002) The evolution of reproductive isolation in spatially structured populations. *Evolution*, **57**, 372–383.

Clement M, Posada D, Crandall K (2000) TCS: a computer program to estimate gene genealogies. *Molecular Ecology*, **9** (10), 1657–1660.

Emelianov I, Marec F, Mallet J (2003) Genomic evidence for divergence with gene flow in host races of the larch budmoth. *Proceedings of the Royal Society of London. Series B, Biological Sciences*, **271**, 97–105.

Excoffier L, Smouse PE, Quattro JM (1992) Analysis of molecular variance inferred from metric distances among DNA haplotypes:

application to human mitochondrial DNA restriction data. *Genetics*, **131**, 479–491.

Friar EA, Boose DL, LaDoux T, Roalson EH, Robichaux RH (2001) Population structure in the endangered Mauna Loa silversword, *Argyroxiphium kauense* (Asteraceae), and its bearing on reintroduction. *Molecular Ecology*, **10**, 1657–1663.

Friar EA, Cruse-Sanders JM, McGlaughlin ME (2007) Gene flow in *Dubautia arborea* and *D. ciliolata*: the roles of ecology and isolation by distance in maintaining species boundaries despite ongoing hybridization. *Molecular Ecology*, doi: 10.1111/j.1365-294X.2007.03423.x.

Friar EA, LaDoux T, Roalson EH, Robichaux RH (2000) Microsatellite analysis of a population crash and bottleneck in the Mauna Kea silversword, *Argyroxiphium sandwicense* ssp. *sandwicense* (Asteraceae), and its implications for reintroduction. *Molecular Ecology*, **9**, 2027–2034.

Friar EA, Robichaux RH, Mount DW (1996) Molecular genetic variation following a population crash in the endangered Mauna Kea silversword, *Argyroxiphium sandwicense* ssp. *sandwicense* (Asteraceae). *Molecular Ecology*, **5**, 687–691.

Fulton M, Hodges SA (1999) Floral isolation between *Aquilegia formosa and A. pubescens*. *Proceedings of the Royal Society of London. Series B, Biological Sciences*, **266**, 2247–2252.

Gillespie JH (2001) Is the population size of a species relevant to its evolution? *Evolution*, **55**, 2161–2169.

Grant PR (1986) *Ecology and Evolution of Darwin's Finches*. Princeton University Press, Princeton, New Jersey.

Grant WS, Bowen BW (1998) Shallow population histories in deep evolutionary lineages of marine fishes: insights from sardines and anchovies and lessons for conservation. *Journal of Heredity*, **89**, 415–426.

Grant PR, Grant BR (1994) Phenotypic and genetic effects of hybridization in Darwin's finches. *Evolution*, **48**, 297–316.

Griswold CK, Baker AJ (2002) Time to the most recent common ancestor and divergence times of populations of common chaffinches (*Fringilla coelebs*) in Europe and North Africa: insights into pleistocene refugia and current levels of migration. *Evolution*, **56**, 143–153.

Hey J, Nielsen R (2004) Multilocus methods for estimating population sizes, migration rates and divergence time, with applications to the divergence of *Drosophila pseudoobscura* and *D. persimilis*. *Genetics*, **167**, 747–760.

Hey J, Wakeley J (1997) A coalescent estimator of the population recombination rate. *Genetics*, **145**, 833–846.

Hey J, Won Y-J, Sivasundar A, Nielsen R, Markert JA (2004) Using nuclear haplotypes with microsatellites to study gene flow between recently separated Cichlid species. *Molecular Ecology*, **13**, 909–919.

Hodges SA (1997) Rapid radiation due to a key innovation in *Aquilegia*. In: *Molecular Evolution and Adaptive Radiation* (eds Givnish TJ, Sytsma KJ), pp. 391–405. Cambridge University Press, Cambridge, UK.

Hudson R, Kreitman M, Aguade M (1987) A test of neutral molecular evolution based on nucleotide data. *Genetics*, **116**, 153–159.

Irschick DJ, Vitt LJ, Zani PA, Losos JB (1998) A comparison of evolutionary radiations in mainland and Caribbean *Anolis* lizards. *Ecology*, **78**, 2191–2203.

Kuhner MK, Yamato J, Felsenstein J (1998) Maximum likelihood estimation of population growth rates based on the coalescent. *Genetics*, **149**, 429–434.

Lack D (1947) *Darwin's Finches*. Cambridge University Press, Cambridge, UK.

Lawton-Rauh AL, Robichaux RH, Purugganan MD (2003) Patterns of nucleotide variation in homoeologous regulatory genes in the allotetraploid Hawaiian silversword alliance (Asteraceae). *Molecular Ecology*, **12**, 1301–1313.

Losos JB, Miles DB (2002) Adaptive radiation in lizards. *American Naturalist*, **160**, 147–157.

MacDonald GA, Abbott AT, Peterson FL (1983) *Volcanoes in the Sea*, 2nd edn. University of Hawaii Press, Honolulu, Hawaii.

Mayr E (1942) *Systematics and the Origin of Species*. Columbia University Press, Cambridge, UK.

McDonald J, Kreitman M (1991) Adaptive protein evolution at the *Adh* locus in *Drosophila*. *Nature*, **351**, 652–654.

Miller RB (1981) Hawkmoths and the geographic patterns of floral variation in *Aquilegia caerulea*. *Evolution*, **35**, 763–774.

Morjan CL, Rieseberg LH (2004) How species evolve collectively: implications of gene flow and selection for the spread of advantageous alleles. *Molecular Ecology*, **13**, 1341–1356.

Nei M (1972) Genetic distance between populations. *American Naturalist*, **106**, 283–292.

Nei M (1987) *Molecular Evolutionary Genetics*. Columbia University Press, New York.

Nielsen R, Wakeley J (2001) Distinguishing migration from isolation: a Markov chain Monte Carlo approach. *Genetics*, **158**, 885–896.

Palsboll PJ, Berube M, Aquilar A, Notarbartolo-di-sciara G, Nielsen R (2004) Discerning between recurrent gene flow and recent divergence under a finite-site mutation model applied to North Atlantic and Mediterranean sea fin whale (*Balaenoptera physalus*) populations. *Evolution*, **58**, 670–675.

Rannala B, Yang Z (2003) Bayes estimation of species divergence times and ancestral population sizes using DNA sequences from multiple loci. *Genetics*, **164**, 1645–1656.

Remington DL, Robichaux RH (2007) Influences of gene flow on adaptive speciation in the *Dubautia arborea–D.ciliolata* complex. *Molecular Ecology*, doi: 10.1111/j.1365-294X.2007.03447.x.

Rieseberg LH, Church SA, Morjan CL (2004) Integration of populations and differentiation of species. *New Phytology*, **161**, 59–69.

Rivera MAJ, Kelley CD, Roderick GK (2004) Subtle population genetic structure in the Hawaiian grouper, *Epinephelus quernus* (Serranidae) as revealed by mitochondrial DNA analyses. *Biological Journal of the Linnean Society*, **81**, 449–468.

Robichaux RH (1984) Variation in the tissue water relations of two sympatric Hawaiian *Dubautia* species and their natural hybrid. *Oecologia*, **65**, 75–81.

Robichaux RH, Canfield JE (1985) Tissue elastic properties of 8 Hawaiian *Dubautia* species that differ in habitat and diploid chromosome-number. *Oecologia*, **66**, 77–80.

Robichaux RH, Carr GD, Liebman M, Pearcy RW (1990) Adaptive radiation of the Hawaiian silversword alliance (Compositae-Madiinae): Ecological, morphological and physiological diversity. *Annals of the Missouri Botanical Garden*, **77**, 64–72.

Robichaux RH, Friar EF, Mount DW (1997) Molecular genetic consequences of a population bottleneck associated with reintroduction of the Mauna Kea silversword (*Argyroxiphium sandwicense* ssp. *sandwicense* [Asteraceae]). *Conservation Biology*, **11**, 1140.

Rozas J, Rozas R (1999) DnaSP version 3: an integrated program for molecular population genetics and molecular evolution analysis. *Bioinformatics*, **15**, 174–175.

Saghai-Maroof M, Soliman KM, Jorgensen R, Allard RW (1984) Ribosomal DNA spacer-length polymorphisms in barley: Mendelian inheritance, chromosomal location, and population dynamics. *Proceedings of the National Academy of Sciences, USA*, **81** (24), 8014–8018.

Saint-Laurent R, Legault M, Bernatchez L (2003) Divergent selection maintains adaptive differentiation despite high gene flow between sympatric rainbow smelt ecotypes (*Osmerus mordax* Mitchill). *Molecular Ecology*, **12**, 315–330.

Schluter D (2000) *The Ecology of Adaptive Radiation*. Oxford University Press, New York.

Tajima F (1989) Statistical method for testing the neutral mutation hypothesis by DNA polymorphism. *Genetics*, **123** (3), 585–595.

Templeton A, Crandall K, Sing C (1992) A cladistic analysis of phenotypic associations with haplotypes inferred from restriction endonuclease mapping and DNA sequence data. III. Cladogram estimation. *Genetics*, **132**, 619–633.

Wang J, Whitlock MC (2003) Estimating effective population size and migration rates from genetic samples over space and time. *Genetics*, **163**, 429–446.

Watterson G (1975) On the number of segregating sites in genetical models without recombination. *Theoretical Population Biology*, **7**, 256–276.

Witter M, Carr GD (1988) Adaptive radiation and genetic differentiation in the Hawaiian silversword alliance (Compositae: Madiianae). *Evolution*, **42**, 1278–1287.

Wright S (1955) Classification of the factors of evolution. *Cold Spring Harbor Symposium on Quantitative Biology*, **20**, 16–24D.

Wright SI, Lauga B, Charlesworth D (2002) Rates and patterns of molecular evolution in inbred and outbred *Arabidopsis*. *Molecular Biology and Evolution*, **19**, 1407–1420.

Wu C-I (2001) The genic view of the process of speciation. *Journal of Evolutionary Biology*, **14**, 851–865.

Yoder AD, Yang Z (2004) Divergence dates for Malagasy lemurs estimated from multiple gene loci: geological and evolutionary context. *Molecular Ecology*, **13**, 757–773.

Zheng X, Arbogast BS, Kenagy GJ (2003) Historical demography and genetic structure of sister species: deermice (*Peromyscus*) in the North American temperate forest. *Molecular Ecology*, **12**, 711–724.

Amy Lawton-Rauh is an Assistant Professor in the Department of Genetics and Biochemistry at Clemson University. She investigates population-level and molecular evolutionary processes shaping genomic variation in plants, including the Hawaiian silversword alliance adaptive radiation and naturally-distributed *Arabidopsis* species. Robert H. Robichaux is a University Distinguished Professor in the Department of Ecology and Evolutionary Biology at the University of Arizona where he studies the ecology, evolution, and conservation genetics of the Hawaiian silversword alliance. Michael D. Purugganan is the Dorothy Schiff Professor of Genomics in the Department of Biology and at the Center for Comparative Functional Genomics at New York University where he studies the evolutionary and ecological genomics of plant adaptation and the genetics of plant domestication.

Appendix I

Nucleotide sequences of *ASAP1-A* haplotypes. Position in alignment is indicated by top numbers. Labels are cross-referenced with specific haplotypes in Fig. 2A. Haplotypes A–R refer to *Dubautia ciliolata* and *Dubautia arborea* haplotypes and haplotypes i–ix refer to *Argyroxiphium sandwicense* haplotypes

```
                  000000000000000000000001111111111111111111111111111111111111111112222
                  000022222233577777888991222233333334444455555555556667777788889999900000
                  012914778956605678237789237913566680015611222235781112456900141245626667
                  285638489053645744830026649025902390835505145828761368772006194433596 87
A                 TAGAGCCGCACTCTCCGCATCCCGTTCTCTAAAAGTGCCGCCCTCAATATTATGCGGTAGATCGAGAAGAG
B                 .................................A...................................
C                 ...G.............................A.............................G......
D                 ..............T.................................................G......
E                 ..............T.........T........................................G......
F                 ..............T.....................T............................G......
G                 ..............T.....................T.....................G.....G......
H                 ................................................G....A.......C.........
I                 .............C..................................G....A.......C.........
J                 .............C..A...............................G....A.......C.........
K                 .............C...A..............................G....A.......C.........
L                 .............C..................................G....A..A....C.........
M                 ......................................C........G....A.......C.........
N                 ......................................C...............................
O                 ...................T..................C...............................
P                 ......................................C.................G.............
Q                 ..C.......AC.........T..CC...-...C.....-.T.......G.........A.........GA
R                 ..C....T..AC......G..T..CC...-...C.....-.T.......G.........A.........GA

i                 C.....G.AG....T....CC..CC.....TTC.....TG..T..GGC...CC.T.....G....A.G.G.
ii                C.....G.AG....T....CC..CC....ATTC.....TG..T..GGC...CC.T.....G.T..A.G.G.
iii               CT....G.AG....T....CC..CC.....TTC.A...TG..T..GGC...CC.TA....G....A.G.G.
iv                CT....G.AG....T....CC..CC.....TTC.A...TGT.T..GGC...CC.TA....G....A.G.G.
v                 CT...AG..G....T....CC..CC..G..TTC....TTG..T..GGC...CC.T.....G..C.A.GAG.
vi                CT..A.G..G..T.T....CC..CC..G..TTC.....TG..T...GC...CC.T.....G....ACG.G.
vii               CT..A.G..G..T.T....CC..CC..G..TTC.....TG..TG..GC...CC.T.....G....ACG.G.
viii              CT....G..G....T....CC.ACC..GG.TTC.....TG..T.TGGC...CC.T.....G....A.G.G.
ix                CT....G..G....T....CC.ACC..GG.TTC.....TG..T.TGGC..CCC.T.....G....A.G.G.
```

Appendix II

Nucleotide sequences of *ASAP1-B* haplotypes. Position in alignment is indicated by top numbers. Labels are cross-referenced with specific haplotypes in Fig. 2B. Haplotypes A–P refer to *Dubautia ciliolata* and *Dubautia arborea* haplotypes. Haplotypes i–xi refer to *Argyroxiphium sandwicense* haplotypes.

```
                    0000000000000000000000011111111111111111111111111111111111122
                    0112233334455666788889922333344444445555555666666777777888900
                    6564507890737778448997903113914455780112789014789123478004502 3
                    9309399179644564630581870192970219516097533585318188469391326 1
A                   TCGGCGCAACAATGAGGCTGAGCGTGATCGTAGAGTCCACGAGACTAGTAGCGTACTTAGGG
B                   .....................................A...................
C                   .....................................................C.....
D                   ..................................T.....................
E                   .....................................................T.......
F                   C....................................................T.......
G                   C.................A..................................T.......
H                   ............T.........T.............................TA......
I                   .A.................A....T.................T......T..T.......
J                   ....................................G...........A...........
K                   ....................T...............G...........A...........
L                   ........................T.........G...........A...........
M                   ........................T.........GT......T...A...........
N                   ......T.................T.........G...........A...........
O                   ......T.....................T......G...........A...........
P                   ......T.............................G....C......A......A....

i                   ..AA....GTTG....A.C.TA..G..A..C.....T.G-.G...G...G...C....GAAA
ii                  ..AA....GTTG....A.C.TA..G..A..C....AT.GT.G...G.......C....GAAA
iii                 ..AA....GTTG....A.C.TA..G..A.AC....AT.GT.G...G.......C....GAAA
iv                  ..AA...GGTTGA.G.A.C.TA..G..A..C..G.AT.GT.G...G.......C....GAAA
v                   ..AA....GTTG....A.C.TA..G..A..C.....T.GT.G...G..A...TC....GAAA
vi                  ..AA...GGTTG....A.C.TA..G..A..C.....T.GT.G...G..A....C....GAAA
vii                 ..AA...GGTTG....A.C.TA..G..A..C.....TTGT.G...G..A....C....GAAA
viii                ..AAG...GTTG....ATC.TA..G..A..C.A...T.GTAG...G.......C....GAAA
ix                  ..AA....GTTG....A.C.TA..GA.A..C.A...T.GT.G...G.A.....C....GAAA
x                   ..AA....GTTG...CA.C.TA..GA.A..C.A...T.GT.G...G.A.....C....GAAA
xi                  ..AA.A..GTTG....A.C.TA..GA.A..C.A...T.GT.G...G.A.....C....GAAA
```

Appendix III

Nucleotide sequences of *ASAP3-A* haplotypes. Position in alignment is indicated by top numbers. Labels are cross-referenced with specific haplotypes in Fig. 2(C). Haplotypes A–U refer to *Dubautia ciliolata* and *Dubautia arbore*a haplotypes and haplotypes i–viii refer to *Argyroxiphium sandwicense* haplotypes.

```
     000000000000000000000000001111111111111222222
     002222455555666666667777774445555566670111122
     247899722499112223671225672494456782660901243 9
     026607489458455691624369087617902603460717338 1

A    TAGGTGT--TGCTACCCGAGACCGGTACGGGATATAACCGAGTGTT
B    ....C..--.....................................
C    .......--...A........A.......................
D    .......--.....T..C.-.........................
E    .......ACC.......C...........................
F    ....C..ACC.......C...........................
G    ....C..ACC.......C.............C...---.GC....
H    ....C..ACC.......CC............C...---.GC....
I    ....CC.ACC.......C.............C...---.GC....
J    C...C..ACC.......C.............C...---.GC....
K    C......ACC.......C.............C...---.GC....
L    .......ACC.......C.............C...---.GC....
M    .......ACC.....T.C.............C...---.GC....
N    .......ACC.......C.............C...---AGC....
O    .......--.....T..C.-...........C...TAT..C....
P    .......--.....T..C.-........A...C.....T..C...C
Q    C......--.....T..C.-...........C.....T..C....
R    C......--.....T..C.-...........C.....T..C..C.
S    C.A....--.....T..C.-...........C.....T..C....
T    C..A...--.....T..C.-...........C........C....
U    ........--.A...T..C.....C.C.T.T..C.G......CC...

I    .......GC...........G...A.......C..-.....C.A.-
ii   .T.....GC...........G...A.......C..-.....C.A.-
iii  .......GC..T....T...G...A.......C..-.....C.A.-
iv   .......GC..T....T...G...A.....T.C..-.....C.A.-
v    .......GC..T....T...G...A.T.....C..-.....C.A.-
vi   .......GC..T....T..AG...A.......C..-.....C.A.-
vii  .......GT..T....T...G...A.......C..-.....C.A.-
viii ......AGC....G......G.T.A......TCG.T.....C.A.-
```

Appendix IV

Nucleotide sequences of *ASAP3-B* haplotypes. Position in alignment is indicated by top numbers. Labels are cross-referenced with specific haplotypes in Fig. 2D. Haplotypes A–C refer to *Dubautia ciliolata* and *Dubautia arborea* haplotypes and haplotypes i–v refer to *Argyroxiphium sandwicense* haplotypes

```
     00000111111111122
     23336446678899902
     72446491174912993
     23025811472584119

A    CGAAACGCAGCTCCTCG
B    ................T
C    ..........A......

i    ..CC.AATTA..AG.T.
ii   ..CCTAATTA..AG.T.
iii  .ACC.AATTA..AG.T.
iv   TACC.AATTA..AG.T.
v    ..CC.AATTA.CAGGT.
```

Appendix V

Nucleotide sequences of *ASCAB9* haplotypes. Position in alignment is indicated by top numbers. Labels are cross-referenced with specific haplotypes in Fig. 2E. Haplotypes A–T refer to *Dubautia ciliolata* and *Dubautia arborea* haplotypes and haplotypes i–iii refer to *Argyroxiphium sandwicense* haplotypes.

```
     00000000000000000000000000000000
     00011112222333444455666667788899
     26623461689458015615127783627815
     00782946991186216194926740630473

A    TTGTACAGGGATAATCCCATTAAGCTTTATGT
B    ......................G..........
C    .......................A........
D    ...............................A.
E    .......A.......................
F    .....T.........................
G    ........A........T.............
H    .C.............................
I    .C.A...........................
J    .C.A.......................C.G...
K    .C.A............T.G.............
L    .C.A......G....................
M    .C.A......G.........C....A.....
N    .C.A..G.............C....A.....
O    ..........G.........C....A.....
P    ....................C...........
Q    ..A...........A.....C...........
R    ....................C.....C.G...
S    C..........CGG.....CC...........
T    C..........CGG.....CC........A..
i    .........A.............C.T..C....
ii   .........A.....T......C.T..C....
iii  ....T....A.............C.T..C...G
```